На основі числових методів квазіконформних відображень проведено математичне моделювання нелінійних процесів витіснення нафтогазової суміші із низькопроникних (типу сланцевих) осадових порід в елементах площового заводнення з урахуванням впливу тріщин гідравлічного розриву. Розроблено алгоритм для проведення числових розрахунків перерозподілу відповідних характеристик: дебітів експлуатаційних свердловин, квазіпотенціалу швидкості фільтрації, координат критичних точок типу призупинки тощо

Ключові слова: числові методи квазіконформних відображень, тріщини гідророзриву, площове заводнення, нелінійні задачі

На основе числовых методов квазиконформных отображений проведено математическое моделирование нелинейных процессов вытеснения нефтегазовой смеси с низкопроницаемых (типа сланцевых) осадочных пород в элементах площадного заводнения с учетом влияния трещин гидравлического разрыва. Разработан алгоритм для проведения численных расчетов перераспределения соответствующих характеристик: дебитов эксплуатационных скважин, квазипотенциалу скорости фильтрации, координат критических точек типа приостановки и тому подобное

Ключевые слова: численные методы квазиконформных отображений, трещины гидроразрыва, площадных заводнения, нелинейные задачи

UDC [519.876.5:530.182]:553.98
DOI: 10.15587/1729-4061.2016.73368

MODELING OF IMPACT OF HYDRAULIC FRACTURES ON THE PROCESS OF FLUID DISPLACEMENT FROM LOW-PERMEABILITY SEDIMENTARY ROCKS

A. Bomba
Doctor of technical sciences,
Professor, Head of the Department*
E-mail: abomba@mail.ru
A. Sinchuk
PhD, Lecturer*
E-mail: sinchukk@mail.ru
*Department of Computer Science and Applied Mathematics
Rivne State Humanitarian University
S. Bandery str., 12, Rivne, Ukraine, 33028

1. Introduction

In oil and gas field development, there are a number of factors that influence the production efficiency. These are both geological characteristics and technical parameters of the reservoir [1]. Much experience in using intensive field development systems has been gained. This applies primarily to pattern waterflooding [2], in which production and injection wells are arranged in a certain way within the corresponding areas.

As it is known, the use of the hydraulic fracturing technology [3, 4] is reasonable in the design of low-permeability (shale) sedimentary rocks and also due to the deterioration of reservoir properties in near-wellbore regions in the course of reservoir development. As a result, fractures extend the area of influence of production wells and form associations with high-permeability zones.

Based on numerical methods for quasiconformal mappings [4–6], the algorithm for solving nonlinear boundary value problems of single-phase filtration in low-permeability sedimentary rocks in the pattern waterflooding elements considering the impact of hydraulic fractures was developed. The algorithm allows predicting the properties of the reservoir system under various impacts and studying the features of filtration in near-wellbore regions. The improvement and development of numerical methods for quasiconformal mappings for mathematical modeling of nonlinear displacement processes in oil reservoirs considering the impact of hydraulic fractures is an urgent issue. This would allow determining the time points of the displacing fluid breakthrough to production wells and complete waterflooding, the coordinates of critical "suspension" points and their quasipotential values, fluid interface position at different time points, the overall filtration rate of production wells, oil fraction dependence, the volume of the fluid displaced in the reservoir within a certain time and, accordingly, the volume of the remaining fluid and so on.

2. Literature review and problem statement

Many scientists around the world to investigate the process of fluid filtering to wells in the presence of hydraulic fractures. In particular, the analytical solution of the relevant boundary value problem, where fractures are presented in the form of a section of zero thickness and finite conductivity is given in [7]. Such a model does not reflect the actual filtration properties of the displacement process, unlike the case where the fracture is modeled in an ellipse form, as in [8]. A more complex model is proposed in [9], which investigated deviations of fractures, depending on the pressure generated by existing microfractures in shale sedimentary rocks. The study of the impact of arrangement of several hydraulic fractures on one production well on the displacement process is proposed in [10]. However, there is the problem of finding a saturation field, which would allow predicting the rate of waterflooding of production wells and identifying the features of operation of a field under the projected arrangement of wells and hydraulic fractures on them.

The results of the mathematical modeling [11] of filtration processes in oil reservoirs with existing hydraulic fractures using numerical methods allow predicting them in general. However, they are insufficient for a proper search of the fluid interface position at different time points, the overall filtration rate of production wells, oil fraction, the volume of the displaced fluid in the reservoir within a certain time, time points of the displacing fluid breakthrough to production well and complete waterflooding, the location of stagnant zones. This problem has been solved partially in [12], which conducted systematic research of mutual impact of fracture parameters and filtration-capacitive characteristics of the environment.

The problems of optimization of the size, permeability coefficient and arrangement of hydraulic fractures have been examined in [13]. The problems of optimization of filtration characteristics of the displacement process in the presence of hydraulic fractures have been solved in [14]. However, these publications did not analyze the locations of so-called "stagnation" zones, depending on the set parameters and arrangement of fractures.

Thus, there is a need to solve a wider range of problems. In addition to the optimum arrangement of injection and production wells, it is necessary to identify efficient arrangement of hydraulic fractures in the vicinities. This would satisfy certain criteria, including by selecting the parameters of hydraulic fractures under constant parameters of the reservoir to achieve the maximum time of water breakthrough to production wells and amount of extracted oil, and the minimum water flow rate.

3. Research goal and objectives

The goal of the research is mathematical modeling of fluid displacement processes in oil reservoirs considering the impact of hydraulic fractures, and development of numerical methods for quasiconformal mappings for solving the relevant boundary value problems of single-phase filtration.

To achieve the goal, the following tasks were set:

– to enhance the mathematical model of fluid displacement from low-permeability (shale) sedimentary rocks in the pattern waterflooding elements in the presence of hydraulic fractures;

– to develop a methodology for solving boundary value problems of filtration processes of displacement from low-permeability (shale) sedimentary rocks considering the impact of hydraulic fractures and related deformation processes in the near-wellbore region when the process under study is described by specially modified Darcy's law regarding the critical value of the pressure gradient under quasistationary filtration flow;

– to develop numerical algorithms for solving relevant boundary value problems, to conduct numerical calculations and analysis of the results on this basis.

4. The method of comprehensive analysis of modeling of nonlinear processes of displacement in oil reservoirs considering the impact of hydraulic fractures

Let us consider the process of single-phase isothermal filtration in horizontal reservoir bed, generated by doubly-symmetric rectilineal rows of injection and production wells, riddled with finite-permeability hydraulic fractures (Fig. 1) without overflows between the respective rows.

Considering the symmetrical arrangement of wells in the reservoir, we have the opportunity to allocate the element $G_z \in \tilde{G}_z$, containing n_* injection wells and one production well with corresponding fractures and their symmetrical parts (Fig. 2, where $d = n_*(r^0 + a)$ – the distance between the separating lines of the symmetry elements, $n_* = 3$, r^0 – the radius of wells, a – half the distance between the injection wells, h – distance between rows).

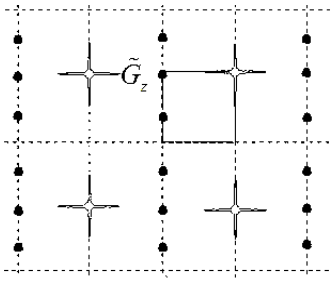

Fig. 1. The diagram of reservoir development with the allocated symmetry element ((●) – injection well, (○) – production well)

When modeling this process, the law of motion and the flow continuity equation, according to [4–6], is represented as:

$$\vec{\upsilon} = -\frac{k\chi(I, I_{kr})}{\mu}\operatorname{grad} p, \quad \operatorname{div}\rho\vec{\upsilon} = 0,$$

under the corresponding conditions on the reservoir boundaries:

$$p\big|_{L_g} = p_*, \quad p\big|_{L^*} = p^*, \quad \frac{\partial p}{\partial n}\Big|_{\tilde{L}} = \frac{\partial p}{\partial n}\Big|_{\tilde{L}} = \frac{\partial p}{\partial n}\Big|_{L_*} = 0 \ (p_* > p^*).$$

Here

$I = I(x,y) = |\operatorname{grad} p(x,y)| = \sqrt{p_x^2 + p_y^2}$ – pressure gradient value p;

$\rho = \rho(p)$ $\vec{\upsilon}$, μ – fluid density, velocity vector and viscosity;

$$k = k(x,y) = \begin{cases} k_\kappa, & (x,y) \in G_z^\kappa, \\ k_0, & (x,y) \in G_z \setminus \bigcup_\kappa G_z^\kappa, \end{cases}$$ – coefficient of absolute permeability of the soil, where

$$G_z^\kappa = \left\{(x,y): \left(\frac{1}{a_\kappa}\cdot\left((x-h)\cos\alpha_\kappa + \left(y - \frac{d}{2}\right)\sin\alpha_\kappa\right)\right)^2 + \right.$$

$$\left. + \left(\frac{1}{b_\kappa}\cdot\left(-(x-h)\sin\alpha_\kappa + \left(y - \frac{d}{2}\right)\cos\alpha_\kappa\right)\right)^2 \le 1\right\}$$

the reservoir area that corresponds to the κ-fracture, $\kappa = 1, 2, 3...$, ($k_\kappa = \text{const}$). Hydraulic fractures are simulated by fragments of ellipses with semiaxes a_κ, b_κ and the corresponding angle of direction – α_κ; L_g, L – boundaries of injection and production wells, respectively, χ – the coefficient characterizing the dependence of permeability of sedimentary rocks (in complicated geological conditions of filtration, for which k_0/μ is a small size) on the pressure gradient value and is determined by the following ratio:

$$\chi(I,I_{kr})=\begin{cases}1+F(I-I_{kr}), \text{at } I>I_{kr},\\ 1, \text{at } I\le I_{kr},\end{cases}$$

where F – monotonically increasing function, I_{kr} – critical value of the initial gradient.

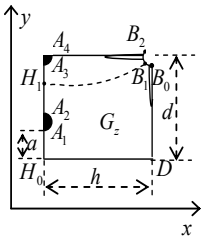

Fig. 2. The symmetry element of the reservoir under pattern waterflooding

To construct an approximate solution of the problem, we introduce the velocity quasipotential in the form of the Laybenson function [5]:

$$\varphi(p)=\varphi_*+\frac{k}{\mu}\int_p^{p_*}\rho(\alpha)d\alpha$$

and rewrite the equation (1) with the corresponding boundary conditions:

$$\operatorname{div}\left(\chi(\tilde I,I_{kr})\operatorname{grad}\varphi\right)=0,\ \ \vec\upsilon=\frac{\chi(\tilde I,I_{kr})}{\tilde\rho(\varphi)}\operatorname{grad}\varphi,$$

$$\varphi\big|_{L_g}=\varphi(p_*)=\varphi_*,\ \ \frac{\partial p}{\partial n}\Big|_{\underset{\sim}{L}}=\frac{\partial p}{\partial n}\Big|_{\tilde L}=\frac{\partial p}{\partial n}\Big|_{L_*}=0,$$

$$\varphi\big|_{L^*}=\varphi(p^*)=\varphi^*,$$

where

$$\tilde\rho(\varphi)=\rho(p(\varphi)),\ \ \tilde I=\frac{\mu}{k\tilde\rho(\varphi)}\sqrt{\varphi_x^2+\varphi_y^2},\ \ \varphi_*<\varphi^*,$$

$$L_g=\{z=x+iy: x=r^0\cos(\theta),\ y=r^0\sin(\theta)+(2g-1)(a+r^0),$$

$$3\pi/2\le\theta\le5\pi/2\}=\{z:\ f_g(x,y)=0,\ g=\overline{1,2}\},$$

$$L^*=\{z=x+iy: x=r^0\cos(\theta)+h,\ y=d/2+r^0\sin(\theta),$$

$$\pi\le\theta\le3\pi/2\}=\{z: f^*(x,y)=0\},$$

$$L_*=A_2A_3=\{z:\ x=0,\ 2r^0+a\le y\le2r^0+3a\},$$

$$\tilde L=A_4B_2=\{z:\ 0\le x\le h,\ y=d\},$$

$$\underset{\sim}{L}=A_1H_0\cup H_0D\cup DB_0=\{z:\underset{\sim}{f}(x,y)=0\},$$

$$A_1H_0=\{z:\ x=0,\ 0\le y\le a\},\ H_0D=\{z:\ y=0,\ 0\le x\le h\},$$

$$DB_0=\{z:\ x=h,\ 0\le y\le d/2\}.$$

Similarly to [4], by introducing the flow function ψ, complex conjugate to φ, the problem of constructing the hydrodynamic grid, determining filtration rate and other specific filtration parameters by the found (fixed at a given time) saturation field is reduced to the quasiconformal mapping $\omega=\omega(z)=\varphi(x,y)+i\psi(x,y)$ of a simply connected region G_z on the corresponding area of complex quasipotential

$$G_\omega=\bigcup_{g=1}^{n_*}G_g\cup\bigcup_{g=1}^{n_*-1}\tilde L_g:$$

$$\frac{\chi(\tilde I,I_{kr})}{\tilde\rho(\varphi)}\frac{\partial\varphi}{\partial x}=\frac{\partial\psi}{\partial y},\ \ \frac{\chi(\tilde I,I_{kr})}{\tilde\rho(\varphi)}\frac{\partial\varphi}{\partial y}=-\frac{\partial\psi}{\partial x},\ (x,y)\in G_z,$$

$$\varphi\big|_{L_g}=\varphi_*,\ \varphi\big|_{L^*}=\varphi^*,\ \psi\big|_{\underset{\sim}{L}}=0,\ \psi\big|_{\tilde L}=Q_{n_*},\ \psi\big|_{L_*}=Q_{u-1},\quad(1)$$

where

$$\upsilon(x,y)=\sqrt{\upsilon_x^2(x,y)+\upsilon_y^2(x,y)},$$

$$G_g=\{\omega:\ \varphi_*<\varphi<\varphi^*,\ Q_{g-1}<\psi<Q_g,\ Q_0=0\},$$

$$\tilde L_g=\{\omega:\ \varphi_{H_g}<\varphi<\varphi^*,\ \psi=Q_g\},$$

$Q_g-Q_{g-1}=\oint_{L_g}-\upsilon_y dx+\upsilon_x dy$ – unknown total filtration rate of injection wells;

$Q=\sum_{g=1}^{n_*}\left(Q_g-Q_{g-1}\right)=Q_{n_*}$ – total flow rate of production wells. Inverse to (1) boundary value problem of quasiconformal mapping $z=z(\omega)=x(\varphi,\psi)+iy(\varphi,\psi)$ of the region G_ω on G_z, and, consequently, the equation for the real $x=x(\varphi,\psi)$ and imaginary $y=y(\varphi,\psi)$ parts of the characteristic flow function is written as:

$$\frac{\chi(\tilde I,I_{kr})}{\tilde\rho(\varphi)}\frac{\partial y}{\partial\psi}=\frac{\partial x}{\partial\varphi},\ \ \frac{\chi(\tilde I,I_{kr})}{\tilde\rho(\varphi)}\frac{\partial x}{\partial\psi}=-\frac{\partial y}{\partial\varphi},\ \ (\varphi,\psi)\in G_\omega,\qquad(2)$$

$$\underset{\sim}{f}(x(\varphi,0),y(\varphi,0))=0,$$

$$\tilde f(x(\varphi,Q_{n_*}),y(\varphi,Q_{n_*}))=0,\ \varphi_*\le\varphi\le\varphi^*,$$

$$f_g(x(\varphi_*,\psi),y(\varphi_*,\psi))=0,\ Q_{g-1}\le\psi\le Q_g,$$

$$f^*(x(\varphi^*,\psi),y(\varphi^*,\psi))=0,\ 0\le\psi\le Q_{n_*},\ g=\overline{2,n_*},$$

$$x_-(\varphi,Q_{g-1})=0,$$

$$2(g-1)(a+r^0)-a\le y_-(\varphi,Q_{g-1})\le y_{H_{g-1}},$$

$$x_+(\varphi,Q_{g-1})=0,\ y_{H_{g-1}}\le y_+(\varphi,Q_{g-1})\le2(g-1)(a+r^0)+a,$$

$$\varphi_*\le\varphi\le\varphi_{H_{g-1}},\qquad(3)$$

$$\left[\frac{\chi(\tilde I,I_{kr})}{\tilde\rho(\varphi)J}\sqrt{\left(\frac{\partial y}{\partial\psi}\right)^2+\left(\frac{\partial x}{\partial\psi}\right)^2}\cos(\vec\upsilon,\vec n)\right]\Bigg|_{\partial G_\omega^l}=0,\qquad(4)$$

where l=1, 2, 3...,

$$\frac{\partial}{\partial\psi}\left(\frac{\chi(\tilde I,I_{kr})}{\tilde\rho(\varphi)}\frac{\partial x}{\partial\psi}\right)+\frac{\partial}{\partial\varphi}\left(\frac{\tilde\rho(\varphi)}{\chi(\tilde I,I_{kr})}\frac{\partial x}{\partial\varphi}\right)=0,$$

$$\frac{\partial}{\partial\psi}\left(\frac{\chi(\tilde I,I_{kr})}{\tilde\rho(\varphi)}\frac{\partial y}{\partial\psi}\right)+\frac{\partial}{\partial\varphi}\left(\frac{\tilde\rho(\varphi)}{\chi(\tilde I,I_{kr})}\frac{\partial y}{\partial\varphi}\right)=0.\qquad(5)$$

The problem of finding the saturation field (2), according to [4], can be presented as follows:

$$\frac{\partial s}{\partial t}=-\frac{\upsilon^2}{\sigma\bar k}\frac{\partial f}{\partial s}\frac{\partial s}{\partial\varphi},\qquad(6)$$

$$s(x(\varphi_*,\psi),y(\varphi_*,\psi),t)=s_*,$$

$$s(x(\varphi,\psi),y(\varphi,\psi),0)=\tilde{s}(x(\varphi,\psi),y(\varphi,\psi)),$$

$$0\le\psi\le Q,\ \ \varphi_*\le\varphi\le\varphi^*, \qquad (7)$$

where the equation (6) is actually spatially one-dimensional, because the variable ψ appears as a parameter.

The difference analogue and the solution algorithm are built as in [4]. At the initial stage, we find the parameter φ_{H_1}, then we consistently solve a series of intermediate problems, corresponding to Fig. 3.

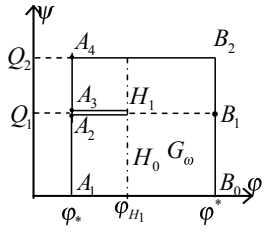

Fig. 3. The region of complex quasipotential

The nodes (φ_i,ψ_j) of the grid area G_ω are determined as follows:

$$\varphi_i=\begin{cases}\varphi_*+i\Delta\varphi_1^g,\ i=\overline{0,n_1^g},\ \Delta\varphi_1^g=(\varphi_{H_g}-\varphi_*)/(n_1^g+1),\\ \varphi_H+(i-n_1^g-1)\Delta\varphi_2^g,\ i=\overline{n_1^g+1,n},\ \Delta\varphi_2^g=(\varphi^*-\varphi_{H_g})/(n_2^g+1),\end{cases}$$

$$\psi_j^g=j\cdot\Delta\psi_g,\ \ (\varphi_i,\psi_j^g)\in G_\omega^g,$$

where

$$j=\overline{\tilde{m}_1,\tilde{m}_2},\ \ \tilde{m}_1=\sum_{l=0}^{g-1}m_l+g-1,$$

$$\tilde{m}_2=\sum_{l=0}^{g}m_l+g-1,$$

$$\Delta\psi_g=(Q_g-Q_{g-1})/m_g,$$

$$m_g=\sum_{l=1}^{g}m_l+g-1,\quad g=\overline{1,n_*},\ \ Q_0=0,$$

$$m_0=0,\ \ n=n_1^g+n_2^g+1,\ \ m=\sum_{l=1}^{n_*}m_l+n_*-1,\ \ m_1,n_1^g,n_2^g\in N.$$

The equation (4) is approximated using the finite volume method [15] as follows:

$$\begin{cases}\gamma^2\left(\dfrac{\chi(\tilde{I}_{i,j+1/2},I_{kr})(x_{i,j+1}-x_{i,j})}{\tilde{\rho}(\varphi_{i,j+1/2})}-\dfrac{\chi(\tilde{I}_{i,j-1/2},I_{kr})(x_{i,j}-x_{i,j-1})}{\tilde{\rho}(\varphi_{i,j-1/2})}\right)+\\ +\dfrac{\tilde{\rho}(\varphi_{i+1/2,j})\left(x_{i+1,j}-x_{i,j}\right)}{\chi(\tilde{I}_{i+1/2,j},I_{kr})}-\dfrac{\tilde{\rho}(\varphi_{i+1/2,j})\left(x_{i,j}-x_{i,j-1}\right)}{\chi(\tilde{I}_{i+1/2,j},I_{kr})}=0,\\ \gamma^2\left(\dfrac{\chi(\tilde{I}_{i,j+1/2},I_{kr})(y_{i,j+1}-y_{i,j})}{\tilde{\rho}(\varphi_{i,j+1/2})}-\dfrac{\chi(\tilde{I}_{i,j-1/2},I_{kr})(y_{i,j}-y_{i,j-1})}{\tilde{\rho}(\varphi_{i,j-1/2})}\right)+\\ +\dfrac{\tilde{\rho}(\varphi_{i+1/2,j})\left(y_{i+1,j}-y_{i,j}\right)}{\chi(\tilde{I}_{i+1/2,j},I_{kr})}-\dfrac{\tilde{\rho}(\varphi_{i-1/2,j})\left(y_{i,j}-y_{i,j-1}\right)}{\chi(\tilde{I}_{i-1/2,j},I_{kr})}=0,\end{cases} \qquad (8)$$

where

$$x_{i,j}=x(\varphi_i,\psi_j),\ \ y_{i,j}=y(\varphi_i,\psi_j),\ \ \varphi_{i,j\pm1/2}=\left(\varphi_{i,j\pm1}+\varphi_{i,j}\right)\Big/2,$$

$$\varphi_{i\pm1/2,j}=\left(\varphi_{i\pm1,j}+\varphi_{i,j}\right)\Big/2,\ \ \tilde{I}_{i,j\pm1/2}=\left(\tilde{I}_{i,j\pm1}+\tilde{I}_{i,j}\right)\Big/2,$$

$$\tilde{I}_{i\pm1/2,j}=\left(\tilde{I}_{i\pm1,j}+\tilde{I}_{i,j}\right)\Big/2,\ \ \tilde{I}_{i,j}=\frac{\mu\sqrt{(x_{i,j+1}-x_{i,j})^2+(y_{i,j+1}-y_{i,j})^2}}{kJ_{i,j}\tilde{\rho}(\varphi_{i,j})\Delta\psi}.$$

Approximations of boundary conditions can be written as:

$$f_g(x_{0,j},y_{0,j})=0,\ j=\overline{\tilde{m}_1,\tilde{m}_2},$$

$$f^*(x_{n,j},y_{n,j})=0,\ j=\overline{0,m},$$

$$x_{i,m_{g-1}}=0,\ \ 2(g-1)(a+r^0)-a\le y_{i,m_{g-1}}\le y_{H_{g-1}},$$

$$x_{i,m_g}=0,\ \ y_{H_g\,1}\le y_{i,m_g}\le 2(g-1)(a+r\ )+a,\ i=\overline{0,n_1},$$

$$\tilde{f}(x_{i,0},y_{i,0})=0,\underline{f}(x_{i,m_p},y_{i,m_p})=0,\ i=\overline{0,n},\ j=\overline{0,m},\ g=\overline{2,n_*}. \qquad (9)$$

Here, as in [6], complex conjugation of harmonic functions $x_{i,j}=x(\varphi_i,\psi_j)$, $y_{i,j}=y(\varphi_i,\psi_j)$ is provided by the conditions of orthogonality of near-boundary normal vectors relative to corresponding tangents along the boundary of the region G_z. Their difference analogues on the well boundaries are as follows:

$$\begin{aligned}&(4x_{1,j}-3x_{0,j}-x_{2,j})(x_{0,j+1}-x_{0,j-1})+\\ &+(4y_{1,j}-3y_{0,j}-y_{2,j})(y_{0,j+1}-y_{0,j-1})=0,\quad j=\overline{\tilde{m}_1,\tilde{m}_2},\\ &(3x_{n,j}+x_{n-2,j}-4x_{n-1,j})(x_{n,j+1}-x_{n,j-1})+\\ &+(3y_{n,j}+y_{n-2,j}-4y_{n-1,j})(y_{n,j+1}-y_{n,j-1})=0,\ \ j=\overline{0,m}.\end{aligned} \qquad (10)$$

Unknown approximate values of flow rate Q_g and potential φ_{H_g} in the flow divergence points in the process of iterations are found by the formulas:

$$\varphi_{H_g}=\varphi_*+(n_1^g+1)\Delta\psi_1\gamma_1^g,\ \ Q_g=m_g\Delta\psi_g,$$

where $\Delta\psi_g=\dfrac{\Delta\varphi_1\gamma_2^g+\Delta\varphi_2\gamma_1^g}{2\gamma_1^g\gamma_2^g}$, and γ_1^g is obtained under "quasiconformal similarity in small" of respective elementary quadrangles of two regions:

$$\gamma_1^g=\sum_{i=0,j=\tilde{m}_1}^{n_1,\tilde{m}_2-1}\frac{\tilde{\rho}(\varphi_{i+1/2,j+1/2})}{\chi(\tilde{I}_{i+1/2,j+1/2},I_{kr})}\frac{\gamma_{i,j}}{m_g(n_1+1)},$$

$$\gamma_2^g=\sum_{i=n_2+1,j=\tilde{m}_1}^{n,\tilde{m}_2-1}\frac{\tilde{\rho}(\varphi_{i+1/2,j+1/2})}{\chi(\tilde{I}_{i+1/2,j+1/2},I_{kr})}\frac{\gamma_{i,j}}{m_gn_2},\ \ g=\overline{1,n_*},$$

$$\gamma_{i,j}=\frac{\tilde{\rho}(\varphi_{i+1/2,j+1/2})}{\chi(\tilde{I}_{i+1/2,j+1/2},I_{kr})}\frac{a_{i,j}+a_{i,j+1}}{b_{i,j}+b_{i+1,j}}, \qquad (11)$$

where

$$a_{i,j}=\sqrt{\left(x_{i+1,j}-x_{i,j}\right)^2+\left(y_{i+1,j}-y_{i,j}\right)^2},$$

$$b_{i,j}=\sqrt{\left(x_{i,j+1}-x_{i,j}\right)^2+\left(y_{i,j+1}-y_{i,j}\right)^2}.$$

The equation (7) is approximated by the "upwind" differencing scheme [4] as follows:

$$\hat{s}_{i,j}=s_{i,j}-\frac{\tau v_{i,j}^2}{\sigma\bar{k}_{i,j}\Delta\varphi_1^g}f'(s_{i-1/2,j})(s_{i,j}-s_{i-1,j}),\ s_{i-1/2,j}=\frac{s_{i,j}+s_{i-1,j}}{2},$$

$$j=\overline{1,m},\ i=\overline{1,n_1^g+1},\ l=1,\ i=\overline{n_1^g+2,n},\ l=2, \qquad (12)$$

where τ – time step, $s_{i,j}$, $\hat{s}_{i,j}$ – saturation at the corresponding time points, $\upsilon_{i,j}$ – velocity. Boundary and initial conditions for saturation in the grid area are as follows: $s_{0,j}=s_*$, $s(x_{i,j},y_{i,j},0)=\tilde{s}(x_{i,j},y_{i,j})$, $j=\overline{0,m}$, $i=\overline{1,n}$.

By setting the step τ, the parameters of partition n_1^g, n_2^g, m_g $g=\overline{1,n_*}$, of the region G_ω and the accuracy ε_1, ε_2 of the algorithm, the initial approximations of coordinates of the boundary nodes (so as to fulfill the condition (8)) and the initial approximations of coordinates of internal nodes ($x_{i,j}^{(0)}$, $y_{i,j}^{(0)}$) according to the formulas (10), we find approximations of values γ_l^g. Then, refinement of coordinates of internal nodes of the hydrodynamic grid by solving (7) with respect to $x_{i,j}$ and $y_{i,j}$ is performed. After that, we correct the boundary nodes with the surrounding boundary and near-boundary nodes fixed using the orthogonality condition, and find the approximation of values Q_g, φ_{H_g}. The conditions for completion of the construction (finding unknown filtration parameters, including the velocity field) algorithm of the hydrodynamic grid in this iterative phase are: stabilization of the flow rate Q_g ($\left|Q_g^{(\kappa+1)}-Q_g^{(\kappa)}\right|<\varepsilon_1$); stabilization of the boundary nodes ($\max\limits_{i,j}\sqrt{(x_{i,j}^{(\kappa)}-x_{i,j}^{(\kappa-1)})^2+(y_{i,j}^{(\kappa)}-y_{i,j}^{(\kappa-1)})^2}<\varepsilon_2$) and so on. In the event of non-compliance with at least one of the conditions, the regions of violation of quasiconformality on the hydrodynamic grid are observed. According to (10), we find new distribution of saturation in the reservoir and repeat the steps of the algorithm using the velocity field and saturation field from the previous iteration step in time (considering the boundary conditions).

5. Numerical calculations of the model problem

Numerical calculations are held at different values of the characteristic parameters that define the geometry of the filtration region when two injection wells account for one production well, provided that $\varphi_*=0$, $\varphi^*=1$, $r^0=0.1$, a=0.8, h=3, d=27, $k_*=1$, $k_\lambda=10$, $\sigma=0.5$, $n_1\times n_2\times m_1\times m_2=4\times20\times25\times25$, $\mu_1=2$, $\mu_2=1$, $\tilde{s}(x,y)=0$, $s_*=1$, $\tau=0.01$. Fig. 4 shows the hydrodynamic grids of the symmetry elements in the initial time point, and Fig. 5 – corresponding saturation distribution at the time point $t=\tilde{t}$ under the following hydraulic fracture parameters: $a_1=b_2=0.1$, $b_1=a_2=1$, $\alpha_1=\pi$, $\alpha_2=3\pi/2$ (Case 1); $a_1=0.1$, $b_1=1$, $\alpha_{1,2}=5\pi/4$ (Case 2); $a_1=0.18$, $b_1=1$, $\alpha=3\pi/2$ (Case 3).

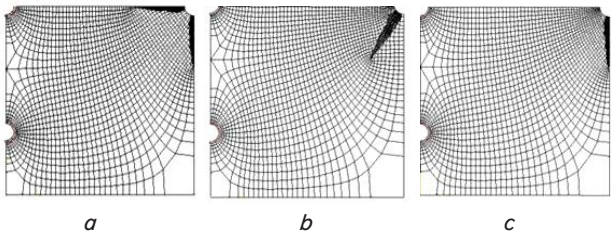

a *b* *c*

Fig. 4. The hydrodynamic grids of the symmetry elements: *a* – in case 1; *b* – in case 2; *c* – in case 3

Fig. 6, 7 show the dependencies of the total filtration rate $Q_{n_*}(t)$ and oil withdrawal values $Q^*(t)$ on the time $t\in[0,t_*]$, respectively, ($t_*=18.62$, further calculation virtually doesn't make sense due to a sharp decline in oil withdrawal) for the above cases.

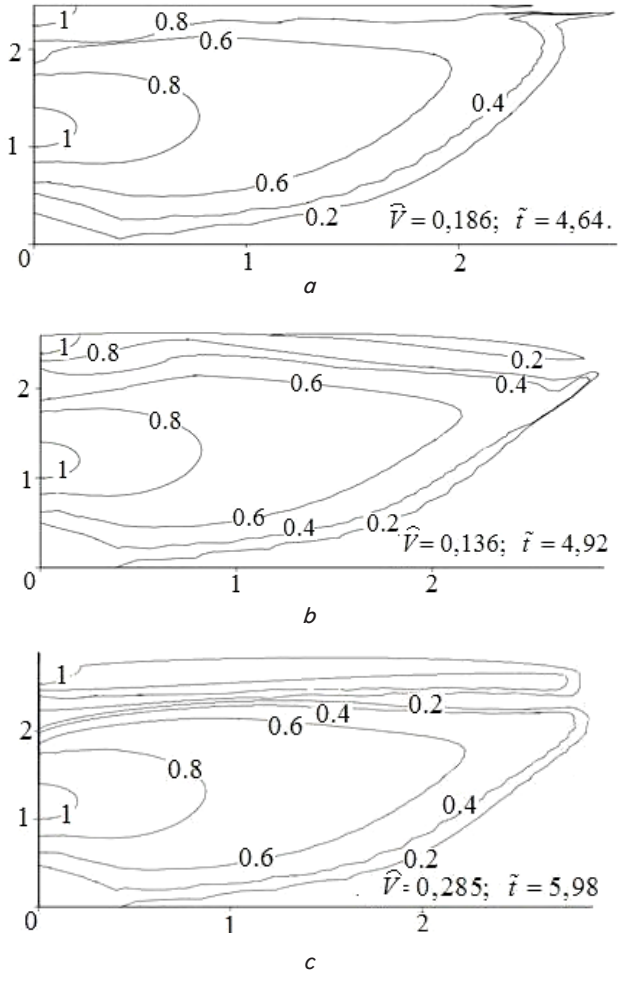

Fig. 5. Saturation distribution of the symmetry elements: *a* – in case 1; *b* – in case 2; *c* – in case 3

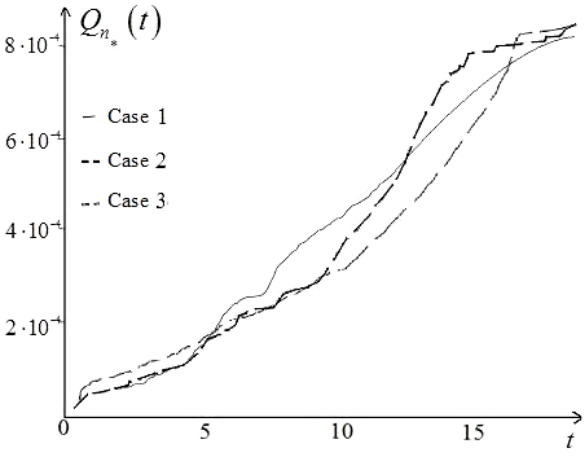

Fig. 6. The graphs of dependence of the total flow rate on the time in the corresponding symmetry elements

According to the calculations, the formulas (4) and (5), the volume of oil in these elements of symmetry before the displacement – V=7.106, and the volume of the oil produced and the residue thereof in the reservoir during the process is $\hat{V}$=3.965, $\check{V}$(18.62)=3.141 (case 1), $\hat{V}$=3.428, $\check{V}$(18.62)=3.678 (case 2), $\hat{V}$=3.789, $\check{V}$(18.62)=3.317 (case 3), respectively.

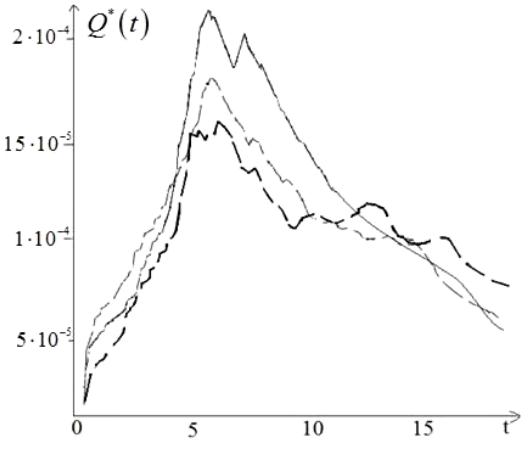

Fig. 7. The graphs of dependence of the oil withdrawal value on the time in the corresponding symmetry elements

6. Discussion of the results of the study of displacement processes in oil reservoirs in the pattern waterflooding elements

In view of the study (computer experiments), we see that the oil withdrawal volume in total filtration rate in each case is reduced differently after reaching the time of displacing reagent breakthrough to the production well. This is due to a significant difference in phase viscosity coefficients, relative phase permeability, parameters and locations of hydraulic fractures. In case 1, there is rapid waterflooding of the production well through one of the fractures and there is a risk of so-called of oil stagnation zones. In case 2, that risk decreases considerably, but the time for complete oil displacement increases. In case 3, we observe too slow course of the oil withdrawal process ("proximity" of withdrawals, especially for cases 1 and 3, is due to equal areas of hydraulic fractures). Also, the fact is confirmed that the "transverse direction" (with respect to injection wells) of hydraulic fractures accelerates the time of the displacing reagent breakthrough to the production well (although provides some growth of oil withdrawal values at the initial stages), and their "longitudinal" direction reduces the number of oil stagnation zones. At the same time, we emphasize that oil stagnation zones in these cases are close to the so-called stagnant zones (areas of reservoirs at the points of which the gradient value is less than some critical value).

The mathematical modeling of low-permeability oil field development allows predicting the rate of waterflooding of production wells and identifying the features of operation under the projected arrangement of wells and hydraulic fractures on them. In these conditions, the problem of optimizing the oil withdrawal process, depending on the given parameters of hydraulic fractures on the production well and determining the location of stagnant zones is solved.

7. Conclusions

The mathematical model of fluid displacement from the low-permeability oil fields in the pattern waterflooding elements in the presence of hydraulic fractures, particularly considering the coefficient that characterizes the dependence of permeability of sedimentary rocks on the pressure gradient value is improved.

Numerical methods for quasiconformal mappings are extended to solve nonlinear boundary value problems of single-phase filtration in low-permeability (shale) sedimentary rocks in the presence of hydraulic fractures. At the same time, the impact of related deformation processes in the near-wellbore region is considered. That is, under quasiconformal filtration flow, the process under study is described by specially modified Darcy's law regarding the critical value of the pressure gradient.

Numerical algorithms for the calculation of filtration characteristics: saturation field, velocity quasipotential, time of the displacing fluid breakthrough to the production well and its complete waterflooding are developed. The algorithm also allows determining the coordinates of the critical "suspension" points and their quasipotential values, fluid interface position at different time points, the overall filtration rate of the production well, the dependence of oil fraction in it. For an effective analysis of the research, calculations of the volume of the fluid displaced in the reservoir within a certain time and the volume of the remaining fluid at an arbitrary time are performed.

References

1. Kanevskaya, R. D. Mathematical modeling of development of oil and gas fields with the use of hydraulic fracturing [Text] / R. D. Kanevskaya. – Moscow: OOO "Core-business centers", 1999. – 212 p.
2. Fazlyev, R. T. Pattern flooding oil fields [Text] / R. T. Fazlyev. – Moscow: Izhevsk, IKI, SIC RHD, 2008. – 256 p.
3. Taleghani, A. D. Analysis of hydraulic fracture propagation in fractured reservoirs: an improved model for the interaction between induced and natural fractures [Text]: PhD Dissertation / A. D. Taleghani. – University of Texas at Austin, 2009. – 216 p.
4. Bomba, A. Ya. Modeling of filtration processes in the oil and gas seams numerical methods quasiconformal mappings [Text]: monograph / A. Ya. Bomba, A. M. Sinchuk, S. V. Yaroschak. – Rivne: LLC «Assol», 2016. – 238 p.
5. Bomba, A. Ya. Mathematic modelling of thermodynamic effects in well bore zone of gas formation under hydraulic fracturing conditions [Text] / A. Ya. Bomba, M. A. Myslyuk, S. V. Yaroschak // Journal of Hydrocarbon Power Engineering. – 2015. – Vol. 2, Issue 1. – P. 1–5.
6. Bomba, A. Ya. Method of complex analysis of modeling of the displacement of oil based coolant effect of hydraulic fracturing [Text] / A. Ya. Bomba, A. M. Sinchuk, S. V. Yaroschak // International scientific journal "System Research and Information Technologies". – 2015. – Vol. 1. – P. 130–140.

7. Astafjev, V. I. Modeling of fluid filtration in the presence of hydraulic fracture formation [Text] / V. I. Astafjev // Bulletin of the Samara State tehnical University. Ser. Sci. Science. – 2007. – Vol. 2, Issue 15. – P. 128–132.
8. Wang, H. Numerical modeling of non-planar hydraulic fracture propagation in brittle and ductile rocks using XFEM with cohesive zone method [Text] / H. Wang // Journal of Petroleum Science and Engineering. – 2015. – Vol. 135. – P. 127–140. doi: 10.1016/j.petrol.2015.08.010
9. Wang, X. Numerical simulation of hydraulic fracturing in orthotropic formation based on the extended finite element method [Text] / X. Wang, F. Shia, H. Liu, H. Wu // Journal of Petroleum Science and Engineering. – 2016. – Vol. 33. – P. 56–69. doi: 10.1016/j.jngse.2016.05.001
10. Abdollahipour, A. Simulating the propagation of hydraulic fractures from a circular wellbore using the displacement discontinuity method [Text] / A. Abdollahipour, M. F. Marji, A. Ya. Bafghi, J. Gholamnejad // International Journal of Rock Mechanics and Mining Sciences. – 2015. – Vol. 80. – P. 281–291. doi: 10.1016/j.ijrmms.2015.10.004
11. Miehe, Ch. Crack driving forces in hydro-poro-elasticity and hydraulic fracturing of fluid-saturated porous media [Text] / Ch. Miehe, S. Mauthe // Computer methods in applied mechanics and engineering. – 2016. – Vol. 304. – P. 619–655.
12. Salimzadeh, S. A three-phase XFEM model for hydraulic fracturing with cohesive crack propagation [Text] / S. Salimzadeh, N. Khalili // Computers and Geotechnics. – 2015. – Vol. 69. – P. 82–92. doi: 10.1016/j.compgeo.2015.05.001
13. Jahandideh, A. Optimization of hydraulic fracturing design under spatially variable shale fracability [Text] / A. Jahandideh, B. Jafarpour // Journal of Petroleum Science and Engineering. – 2016. – Vol. 138. – P. 174–188. doi: 10.1016/j.petrol.2015.11.032
14. Zhang, Sh. Determination of in situ stresses and elastic parameters from hydraulic fracturing tests by geomechanics modeling and soft computing [Text] / Sh. Zhang, Sh. Yin // Journal of Petroleum Science and Engineering. – 2014. – Vol. 124. – P. 484–492. doi: 10.1016/j.petrol.2014.09.002
15. Samarskiy, A. A. The theory of difference schemes [Text] / A. A. Samarskiy. – Moscow: Nauka, 1983. – 616 p.